Geometry dependent current-voltage characteristics of ZnO nanostructures: A combined nonequilibrium Green's function and density functional theory study

Zhiwen Yang,[1] Bin Wen,[1,a)] Roderick Melnik,[2] Shan Yao,[1] and Tingju Li[1]
[1]*School of Materials Science and Engineering, Dalian University of Technology, Dalian, Liaoning 116023, People's Republic of China*
[2]*M²NeT Laboratory, Wilfrid Laurier University, Waterloo, 75 University Ave. West, Ontario N2L 3C5, Canada*

(Received 17 July 2009; accepted 14 October 2009; published online 9 November 2009)

Current-voltage (I-V) characteristics of different ZnO nanostructures were studied using a combined nonequilibrium Green's function and density functional theory techniques with the two-probe model. It was found that I-V characteristics of ZnO nanostructures depend strongly on their geometry. For wurtzite ZnO nanowires, currents decrease with increasing lengths under the same applied voltage conditions. The I-V characteristics are similar for single-walled ZnO nanotubes and triangular cross section ZnO nanowires but they are different from I-V characteristics of hexagonal cross section ZnO nanowires. Finally, our results are discussed in the context of calculated transmission spectra and densities of states. © *2009 American Institute of Physics*.
[doi:10.1063/1.3259657]

Semiconductor nanostructures have been generating tremendous research interests in the past years due to their unique properties and important applications in mesoscopic physics, biology and medicine, and fabrication of nanoscale electronic and photonic devices.[1,2] In particular, as a typical semiconductor, Zinc oxide (ZnO) has been widely utilized in the development of electronic and photonic devices owing to its wide direct bandgap (3.37 eV) and large exciton binding energy (60 meV).[3,4] In recent years, various ZnO nanostructures, including nanowires, nanowire arrays, nanorings, nanobelts, and nanobridges,[5–7] have been synthesized. Among other applications areas, they have also emerged as promising candidates for quantum devices, such as blue light-emitting diodes, field-effect transistors, piezoelectric antenna arrays as well as nanocantilevers, etc.[8–11] Given these applications, it is very important to understand the current-voltage (I-V) characteristics for these ZnO nanostructures.

Several experimental works have already been carried out to understand the I-V characteristics of ZnO nanostructures.[8,12–14] For example, various aspects such as air pressure,[8,13] temperature,[11–14] ultraviolet irradiation,[12] contact between ZnO nanostructures and electrodes,[13] and gas ambient effects on I-V characteristics[14] have been investigated. While most theoretical works on ZnO nanostructures have had a focus on their binding energies,[15–18] highest occupied molecular orbital-lowest unoccupied molecular orbital gaps,[15,18] band structures,[16] elasticity,[17] stability,[16,18] there have been only a few reports on their electrical characteristics.[16] Although geometry dependence of I-V characteristics has been studied in the past for other types of nanowires with density functional models,[19,20] a geometry dependent I-V characteristics of ZnO nanostructures have not been studied in detail experimentally and theoretically to date. We will address this issue by using state-of-the-art calculations based on density functional theory (DFT) combined with nonequilibrium Green's function (NGF) technique.[21–24]

Here, three cross sections of ZnO nanostructures were considered, namely, hexagonal and triangular cross section ZnO nanowires (ZnO-NWs), and single-walled ZnO nanotube (ZnO-SWNT). The initial hexagonal and triangular cross section ZnO-NWs were directly cut from a large wurtzite (WZ) ZnO supercell along the [0001] direction. The conventional ZnO-SWNT was modeled in analogy with a 6 $\times$6 single-walled boron-nitrogen nanotube. First, geometry optimizations were performed for these nanostructures using the DFT with the effective core potentials implemented in the DMOL package.[25] We used a double numerical basis including *p*- and *d*-polarization functions and adopted the generalized gradient approximation with the Perdew and Wang (PW91) parameterization[26] to describe the exchange-correlation interaction. Using the optimized ZnO nanostructures as input structures, the I-V characteristics have been studied using DFT and NGF combined with the two-probe model (electrode-nanostructure-electrode) implemented in ATOMISTIX TOOLKIT package.[21–24] As shown in Fig. 1, ZnO nanostructures are coupled between two lithium electrodes, and this method has already been utilized in several compu-

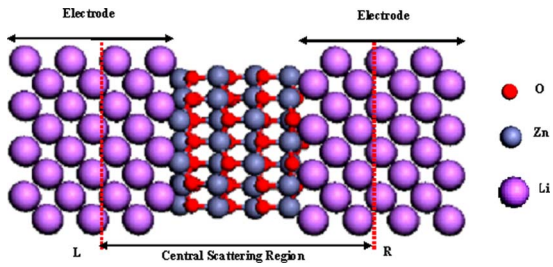

FIG. 1. (Color online) ZnO nanostructure coupled between two lithium (001) surfaces of electrodes. L and R label the left and right electrodes, respectively. Vertical dotted lines represent borders of the central scattering region.

a)Author to whom correspondence should be addressed. Electronic mail: wenbin@dlut.edu.cn.

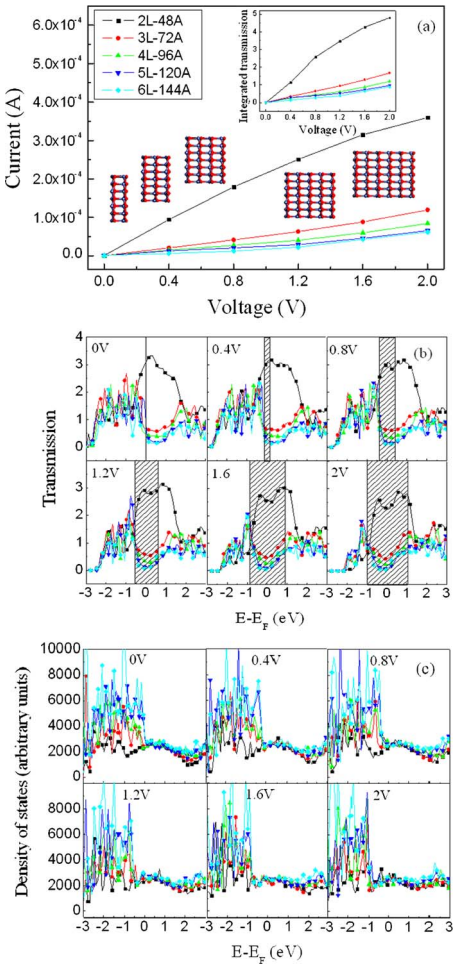

FIG. 2. (Color online) (a) Current-voltage curves (inset figure shows the relationship between integrated transmissions and voltage), (b) transmission spectra, (c) densities of states of hexagonal cross section ZnO-NWs with different lengths.

tational studies.[27–29] The atomic distance between the ZnO nanostructure and the electrode has been explicitly optimized through calculating the total energy of each system. I-V characteristics have been calculated with the Landauer formula[30]

$$I = \frac{2e^2}{h}\int T(E,V_b)[f_1(E) - f_r(E)]dE,$$

where e is the electron charge, h is Planck's constant, and $f_1(E)$, $f_r(E)$ represent the Fermi distribution functions at the left and right electrodes, respectively. $T(E,V_b)$ stands for the transmission coefficient as a function of the electron energy E and bias voltage V_b. In our computational scheme, periodic boundary conditions have been used when solving Poisson's equation and the convergence in total energy tolerance was 0.0001 eV.

In order to understand the effect of geometry on the I-V characteristics of ZnO nanostructures, the I-V curves have been calculated for hexagonal cross section (68.7 Å^2) WZ ZnO-NWs with different lengths under the electrodes temperature of 300 K. The smallest hexagonal cross section WZ ZnO nanowire containing 48 atoms of four layers (two Zn-O double layers). Larger ZnO-NWs are generated by repeating the nanowire along the [0001] direction. Similar to Ref. 15, we denote them as 2L-48A, 3L-72A, 4L-96A, 5L-120A, and 6L-144A, respectively. As can be seen from Fig. 2(a), for all ZnO-NWs, the I-V curves increase monotonously with the bias voltage increasing. Under the same applied voltage conditions, 2L-48A ZnO nanowire current is larger than that of other ZnO-NWs. To further study the results, transmission spectra have been calculated, and shown in Fig. 2(b). The shaded area represents the bias window, which is referred to the energy interval from the chemical potential of the left electrode to that of the right electrode. Resonant transmission peaks refer to the conducting channels. That is, the higher integrated transmissions in the bias window, the higher the current. It is clearly seen that the 2L-48A ZnO nanowire has larger integrated transmissions in the bias window, and lead to larger current values. For all ZnO-NWs, more resonant transmission peaks shift into the bias window with increasing voltages, which explains the monotonous increase of the I-V curves. In addition, integrated transmissions have been calculated for different bias windows, and inserted in Fig. 2(a). By comparing these integrated transmission-voltage relationships with the corresponding current-voltage relationships, an analogous trend has been found. Figure 2(c) shows the density of states (DOS) of this under applied voltages from 0 to 2 V. It can be seen that there are electrons at the Fermi level. The order of magnitude for electron Fermi wavelength in ZnO-NWs is a few tenths of nanometers,[31,32] and it is close to ZnO-NWs geometry size, indicating that electron scattering effects exist. Increasing lengths of the multiconducting channel system[32,33] result in an increase of the electron scattering effect and it is the main reason for the current decrease with increasing nanowire lengths under the same applied voltage conditions. For the 2L-48A ZnO nanowire, ballistic transport is dominant. Therefore, it has a larger current value than other larger nanowires under the same applied voltage conditions and I-V curves show sublinearity. But for the other ZnO nanowires, the scattering effect is dominant, hence I-V curves show superlinearity.

Shapes dependent I-V characteristics of ZnO nanostructures have also been studied. Three ZnO nanostructures with different cross sections and nearly the same length; hexagonal (68.7 Å^2) and triangular (47.7 Å^2) cross section ZnO-NWs and ZnO-SWNT (40.8 Å^2), have been analyzed. Their optimized lengths are 1.128, 1.125, and 1.059 nm, respectively. The relationships between current and voltage for various shapes of ZnO nanostructures are plotted in Fig. 3(a). The I-V characteristics of ZnO-SWNT are similar to those of triangular cross section ZnO-NWs. For hexagonal cross section ZnO-NWs, under the same applied voltage conditions, current is lower than those of ZnO-SWNT and triangular cross section ZnO-NWs. Our results also indicated that with an increase in voltage, the I-V curves of ZnO-SWNT and triangular cross section ZnO-NWs intersect, and the cross point is at 1.4 V. The corresponding transmission spectra of ZnO nanostructures have been calculated to further analyze the difference, and they are shown in Fig. 3(b). It can be seen that each of the three ZnO nanostructures has a significant resonant transmission peak contributing to the current near the Fermi level. We denote these peaks as Pn, Pt, and Ph for ZnO-SWNT, triangular, and hexagonal cross section ZnO-NWs, respectively. The Pt peak is larger than that of Pn peak when the applied voltage arrives at 1.6 V, which is the direct reason for the intersection of I-V curves of ZnO-SWNT and triangular cross section ZnO-NWs. Moreover, calculated integrated transmissions for different bias windows are inserted in Fig. 3(a). It is also found that an analogous trend

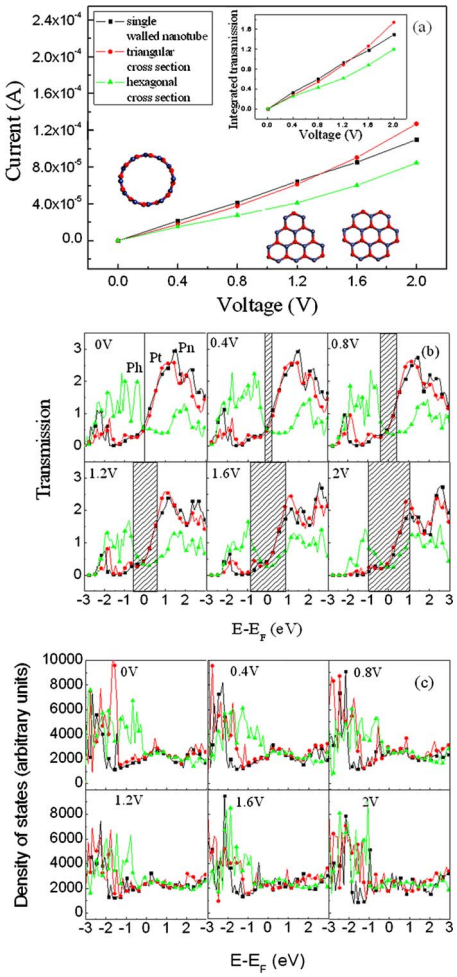

FIG. 3. (Color online) (a) Current-voltage curves (inset figure shows the relationship between integrated transmissions and voltage), (b) transmission spectra, (c) densities of states of ZnO nanostructures with different shapes.

has been shown between the integrated transmission-voltage relationships with the corresponding current-voltage relationships. DOS for our three ZnO nanostructures have also been calculated, and plotted in Fig. 3(c). It can be seen that DOS values for hexagonal cross section ZnO-NWs near the Fermi level are larger than those of ZnO-SWNT and triangular cross section ZnO-NWs. Since lengths of the optimized ZnO nanostructures are almost equivalent, the I-V characteristics difference can be attributed to the cross section shape. Due to scattering effects, the channel transmissions decrease with the increasing of the cross sectional area.[32,33] Therefore, the larger cross sectional area leads to more electrons being reflected.

In conclusion, using NGF and DFT techniques combined with the two-probe model, geometry dependent I-V characteristics have been investigated for three kinds of ZnO nanostructures: hexagonal and triangular cross section ZnO-NWs, and the ZnO-SWNT. For ZnO-NWs, under the same applied voltage conditions the current decreases with increasing lengths. The I-V characteristics of ZnO-SWNT are similar to those of triangular cross section ZnO-NWs. For hexagonal cross section ZnO-NWs, under the same applied voltage conditions, the current is lower than those of ZnO-SWNT and triangular cross section ZnO-NWs. Finally, our results have been discussed in the context of calculated transmission spectra and densities of states.

This work was supported by the NNSF of China (Grant Nos. 50772018 and 50402025) and the Program for NCET in Universities of China (Grant No. NCET-07-0139). R.M. acknowledges support from the NSERC and CRC program. B.W. acknowledges computational support from Professor J. J. Zhao of Dalian University of Technology of China.

[1]B. P. Zhang, N. T. Binh, and Y. Segawa, Appl. Phys. Lett. **84**, 586 (2004).
[2]B. Wen and R. Melnik, Appl. Phys. Lett. **92**, 261911 (2008).
[3]Y. R. Ryu, T. S. Lee, J. A. Lubguban, Y. S. Park, and C. J. Youn, Appl. Phys. Lett. **87**, 153504 (2005).
[4]I. Shalish, H. Temkin, and V. Narayanamurti, Phys. Rev. B **69**, 245401 (2004).
[5]Z. L. Wang and J. Song, Science **312**, 242 (2006).
[6]X. Y. Kong, Y. Ding, R. Yang, and Z. L. Wang, Science **303**, 1348 (2004).
[7]J. F. Conley, L. Stecker, and Y. Ono, Appl. Phys. Lett. **87**, 223114 (2005).
[8]Z. Y. Fan, D. W. Wang, P. C. Chang, W. Y. Tseng, and G. Jia Lu, Appl. Phys. Lett. **85**, 5923 (2004).
[9]X. D. Wang, C. J. Summers, and Z. L. Wang, Nano Lett. **4**, 423 (2004).
[10]M. H. Zhao, Z. L. Wang, and S. X. Mao, Nano Lett. **4**, 587 (2004).
[11]C. S. Lao, J. Liu, P. X. Gao, L. Y. Zhang, D. Davidovic, R. Tummala, and Z. L. Wang, Nano Lett. **6**, 263 (2006).
[12]O. Harnack, C. Pacholski, H. Weller, A. Yasuda, and J. M. Wessels, Nano Lett. **3**, 1097 (2003).
[13]Q. H. Li, Q. Wan, Y. X. Liang, and T. H. Wang, Appl. Phys. Lett. **84**, 4556 (2004).
[14]Y. W. Heo, L. C. Tien, D. P. Norton, B. S. Kang, F. Ren, B. P. Gila, and S. J. Pearton, Appl. Phys. Lett. **85**, 2002 (2004).
[15]C. Li, W. L. Guo, Y. Kong, and H. J. Gao, Appl. Phys. Lett. **90**, 223102 (2007).
[16]Z. Zhou, Y. F. Li, L. Liu, Y. S. Chen, S. B. Zhang, and Z. F. Chen, J. Phys. Chem. C **112**, 13926 (2008).
[17]Z. C. Tu and X. Hu, Phys. Rev. B **74**, 035434 (2006).
[18]B. Wen and R. Melnik, Chem. Phys. Lett. **466**, 84 (2008).
[19]N. Radulovic, M. Willatzen, R. V. N. Melnik, and L. C. L. Y.Voon, J. Comput. Theor. Nanosci. **3**(4), 551 (2006).
[20]N. Radulovic, M. Willatzen, and R. V. N. Melnik, Computational Science and Its Applications (ICCSA 2004, Part 3) **3045**, 817 (2004).
[21]ATOMISTIX TOOLKIT, Version 200810, Quantumwise A/S www.quantumwise.com.
[22]M. Brandbyge, J. L. Mozos, P. Ordejon, J. Taylor, and K. Stokbro, Phys. Rev. B **65**, 165401 (2002).
[23]J. M. Soler, E. Artacho, J. D. Gale, A. Garcia, J. Junquera, P. Ordejon, and D. Sanchez-Portal, J. Phys.: Condens. Matter **14**, 2745 (2002).
[24]J. Taylor, H. Guo, and J. Wang, Phys. Rev. B **63**, 245407 (2001).
[25]B. Delley, J. Chem. Phys. **92**, 508 (1990).
[26]J. P. Perdew and Y. Wang, Phys. Rev. B **45**, 13244 (1992).
[27]L. P. Zhou, S. W. Yang, M. F. Ng, M. B. Sullivan, V. B. C. Tan, and L. Shen, J. Am. Chem. Soc. **130**, 4023 (2008).
[28]K. Odbadrakh, P. Pomoriski, and C. Roland, Phys. Rev. B **73**, 233402 (2006).
[29]Z. Crljen, A. Grigoriev, G. Wendin, and K. Stokbro, Phys. Rev. B **71**, 165316 (2005).
[30]M. Büttiker, Y. Imey, R. Landauer, and S. Pinhas, Phys. Rev. B **31**, 6207 (1985).
[31]B. J. van Wees, H. van Houten, C. W. J. Beenakker, J. G. Williamson, L. P. Kouwenhoven, D. van Marel, and C. T. Foxon, Phys. Rev. Lett. **60**, 848 (1988).
[32]M. Brandbyge, M. R. Sorensen, and K. W. Jacobsen, Phys. Rev. B **56**, 14956 (1997).
[33]M. Brandbyge, K. W. Jacobsen, and J. K. Norskov, Phys. Rev. B **55**, 2637 (1997).